

# COMPARISON OF QUADRUPOLE SCAN AND MULTI-SCREEN METHOD FOR THE MEASUREMENT OF PROJECTED AND SLICE EMITTANCE AT THE SwissFEL INJECTOR TEST FACILITY

M. Yan\*, Ch. Gerth, DESY, Hamburg, Germany  
 B. Beutner†, R. Ischebeck, E. Prat, PSI, Villigen, Switzerland

## Abstract

High-brightness electron bunches with small transverse emittance are required to drive X-ray free-electron lasers (FELs). For the measurement of the transverse emittance, the quadrupole scan and multi-screen methods are the two most common procedures. By employing a transverse deflecting structure, the measurement of the slice emittance becomes feasible. The quadrupole scan is more flexible in freely choosing the data points during the scan, while the multi-screen method allows on-line emittance measurements utilising off-axis screens in combination with fast kicker magnets. The latter is especially the case for high-repetition multi-bunch FELs, such as the European X-ray Free-Electron Laser (XFEL), which offer the possibility of on-line diagnostics. In this paper, we present comparative measurements of projected and slice emittance applying these two methods at the SwissFEL Injector Test Facility and discuss the implementation of on-line diagnostics at the European XFEL.

## INTRODUCTION

Control and optimization of the transverse emittance as well as the slice emittance of the driving electron bunch are crucial to the performance of X-ray free-electron lasers (FEL). The principle of emittance measurement is described, for instance, in detail in Ref. [1]. The emittance to be reconstructed at a reference point is based on the second-order beam moments with  $\epsilon^2 = \langle x_0^2 \rangle \cdot \langle x_0'^2 \rangle - \langle x_0 x_0' \rangle^2$ . Transportation of the beam moments to a downstream position using the transport matrix  $R$  yields the relation

$$\langle x^2 \rangle = R_{11}^2 \langle x_0^2 \rangle + 2R_{11}R_{12}\langle x_0 x_0' \rangle + R_{12}^2 \langle x_0'^2 \rangle. \quad (1)$$

The squared beam size  $\langle x^2 \rangle$  can be accessed directly using observation screens. At least three measurements for three different transport matrices  $R$  are required to obtain the second-order beam moments at the reference point. Commonly, linear least squares method is employed for the fit to the equation system. The same procedure can be adapted for the  $y$ -plane.

Variation of the transport matrices can be achieved with the quadrupole scan or multi-screen method. In the quadrupole scan method, the measurement point is fixed and the strengths of the quadrupoles between the reconstruction and measurement point are changed. In the multi-screen

method, the measurement point is chosen at different downstream locations to provide various transport lattices.

The quadrupole scan is more flexible in arranging data points, but cannot be performed in parallel to the FEL operation. The multi-screen method requires more space and diagnostic stations, but provides the possibility of parasitic emittance measurements utilizing off-axis screens. Such online diagnostics are highly demanded at high repetition multi-bunch FEL, such as the European XFEL [2]. A comparison of different aspects of these two methods is studied in Ref. [3].

Combined use of a transverse deflecting structure (TDS) with these two methods allows for measurement of the slice emittance. The longitudinal coordinate of the bunch is translated by the TDS to one transverse direction. The emittance in the other transverse plane perpendicular to the streak direction can then be determined in a time-resolved domain. Careful consideration in the accelerator optics has to be taken into account for the time resolution, which is correlated inversely to the TDS streak parameter [4]

$$S \sim \frac{eV_0 k}{pc} \sqrt{\beta_y, \text{TDS}} \cdot \sin(\Delta\mu_y). \quad (2)$$

Comparative measurements of projected and slice emittance using these two methods have been conducted at the SwissFEL Injector Test Facility (SITF) at PSI in Switzerland. In this paper, the experimental setup is described and the results are discussed.

## DIAGNOSTIC SECTION

One main purpose of the SITF [5] is to demonstrate the feasibility of the SwissFEL. A schematic layout of the SITF is shown in Fig. 1. The nominal beam energy is 250 MeV and the charge can be varied from 10 pC to 200 pC.

The diagnostic section for the comparative emittance measurement is located downstream of the bunch compressor at a nominal energy of 250 MeV. An S-band TDS streaks the bunch in the vertical direction and enables slice emittance measurement in the horizontal plane. The TDS is followed by several matching quadrupoles, a 3.5-cell FODO section with multiple standard screen stations and a high-resolution transverse profile monitor [6]. The screen stations inside the FODO section are equipped with optical transition radiation (OTR) screens. The high-resolution profile monitor, which employs a scintillator screen, is designed in a special configuration to achieve resolution much smaller than the thickness of the scintillator and more robust than the OTR screen for operation with low charge bunches due to its higher light

\* minjie.yan@desy.de

† Now at Deutsches-Elektronen Synchrotron DESY

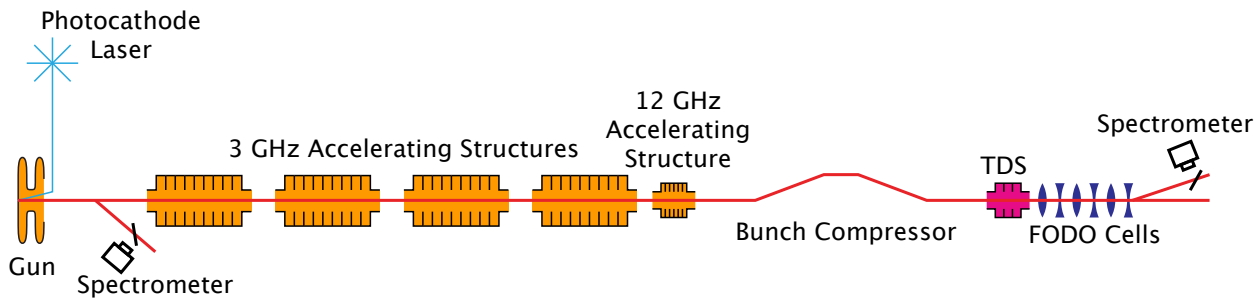


Figure 1: Schematic layout of the SwissFEL Injector Test Facility. The diagnostic section for emittance measurement, comprising S-band TDS, matching quadrupoles and FODO section, is located downstream of the bunch compressor.

yield. Hence, the high-resolution profile monitor was chosen for the quadrupole scan method, which has flexibility in selecting the measurement screens.

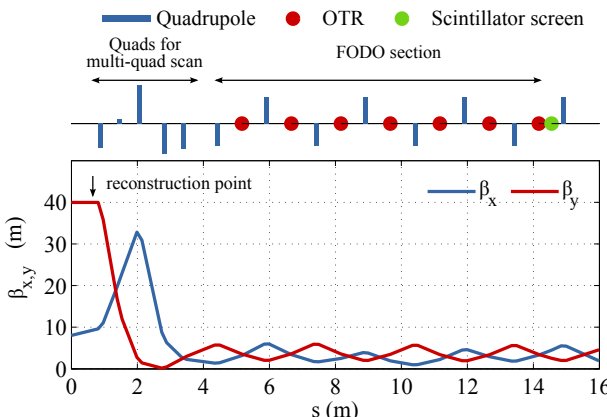


Figure 2: Accelerator optics (starting from the TDS) used for the multi-screen method. The same optics is used for both projected and slice emittance measurement.

Figure 2 shows the beamline layout of the diagnostic section starting from the TDS (top) and the design optics for the multi-screen method (bottom). The same optics is used for both projected and slice emittance measurement. From the TDS, where a large  $\beta_y$  in the streaking direction is essential to a good time resolution (see Eq. 2), the beam is matched with help of five quadrupoles into the 3.5-cell quasi-symmetric FODO section with phase advances of  $72^\circ$  and  $52^\circ$  in each cell in x and y plane, respectively. The reconstruction point for the slice emittance and its value of twiss parameters are the same as those in the multi-screen method, which makes additionally a comparison of the reconstructed optics using these two methods possible. The phase advances for the measurement of slice emittance are illustrated in Fig. 3 (right). With the combined use of the five quadrupoles, the horizontal phase advance  $\Delta\mu_x$  covers from  $30^\circ$  to  $180^\circ$  with equal steps and a constant  $\Delta\mu_y = 90^\circ$  for the maximum streaking effect of TDS can be achieved. The multi-quadrupole scan has been used routinely for optimizing the slice emittance at the SITF [8].

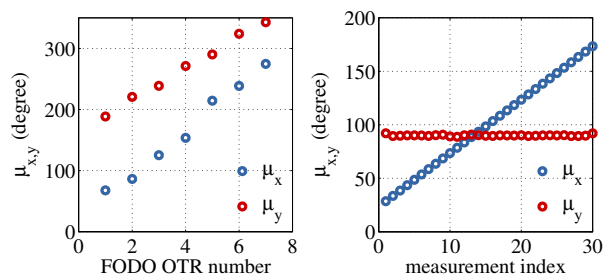


Figure 3: Phase advances from TDS to the individual measurement point for (left) projected and slice emittance measurement using multi-screen method, and (right) slice emittance measurement using quadrupole scan method.

The high-resolution profile monitor used for the quadrupole scan method is installed at the end of the FODO section and denoted with a green dot in Fig. 2. One single quadrupole (the fifth quadrupole in Fig. 2) is scanned for the measurement of projected emittance, covering phase advances in total of about  $180^\circ$  in both x and y planes [7]. Five quadrupoles (the first five quadrupoles in Fig. 2) are employed together for the measurement of slice emittance. The reconstruction point for the slice emittance and its value of twiss parameters are the same as those in the multi-screen method, which makes additionally a comparison of the reconstructed optics using these two methods possible. The phase advances for the measurement of slice emittance are illustrated in Fig. 3 (right). With the combined use of the five quadrupoles, the horizontal phase advance  $\Delta\mu_x$  covers from  $30^\circ$  to  $180^\circ$  with equal steps and a constant  $\Delta\mu_y = 90^\circ$  for the maximum streaking effect of TDS can be achieved. The multi-quadrupole scan has been used routinely for optimizing the slice emittance at the SITF [8].

## EXPERIMENTAL RESULTS

The comparative measurements were performed using electron bunches with an energy of 200 MeV. All accelerating modules were operated on-crest. A bunch charge of 200 pC was chosen in order to get enough light emission from the streaked bunch using OTR screens. The beam sizes are defined using Gaussian fit to the transverse profiles. The

errors given in this paper include only statistical errors and are determined according to error propagation.

### Projected Emittance

During the measurement using multi-screen method, the images taken with the fourth OTR screen display clear features affected by the OTR point spread function and therefore are omitted for the reconstruction of emittance.

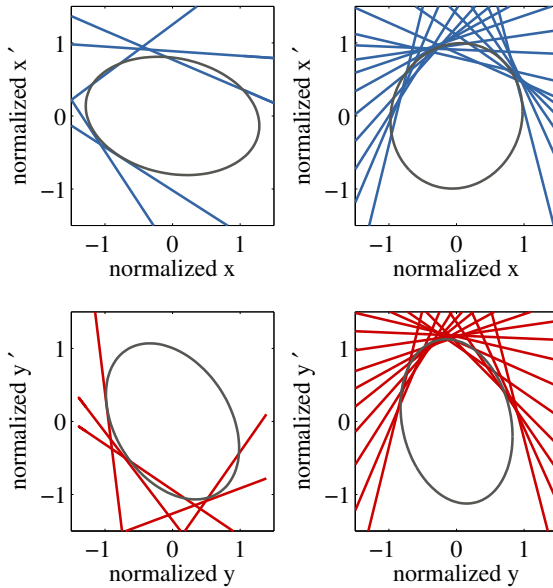


Figure 4: Fits of the beam ellipses using multi-screen method (left) and single quadrupole scan (right) for the measurement of projected emittance. The lines represent each measured beam size.

The results of the projected emittance measurements are shown in Fig. 4, and the reconstructed normalized projected emittances  $\epsilon_N$  together with the mismatch parameters  $B_{\text{mag}}$  [1] are summarized in Table 1. The results obtained with these two methods are comparable, but the normalized emittances derived using the multi-screen method are slightly larger than that using single quadrupole scan in both planes. Errors from optics mismatch are minimized in the single quadrupole scan method, while the mismatch parameters of 1.12 and 1.07 in the multi-screen method indicate that there's still some errors coming from the optics mismatch.

Table 1: Summary of Projected Emittance Measurements

Multi-screen method	Single quad-scan
$\epsilon_{N,x}$	$513 \pm 8 \text{ nm}$
$\epsilon_{N,y}$	$495 \pm 6 \text{ nm}$
$B_{\text{mag},x}$	1.12
$B_{\text{mag},y}$	1.07

### Slice Emittance

The machine was operated with the same settings as for the projected emittance measurement. Several matching

iterations were performed to match the core slice to the design optics. The rms bunch length was determined to be approximately 3 ps. Each slice has a width of one fifth of the bunch length. The core slice is defined as the one at the longitudinal mean position of the bunch.

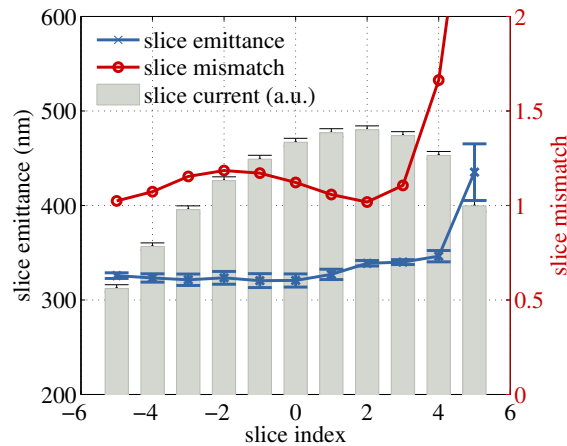
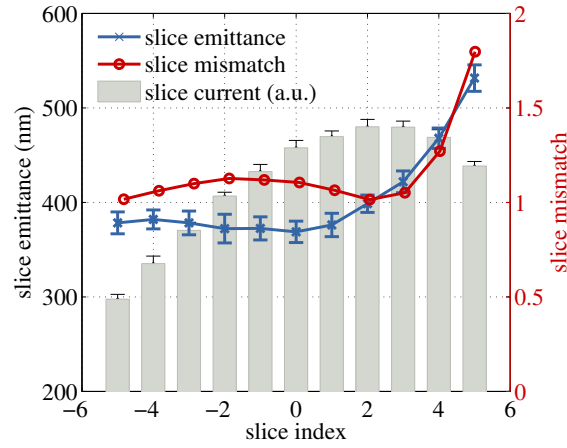


Figure 5: Normalized horizontal slice emittance and slice mismatch parameter obtained with (top) multi-screen method and (bottom) quadrupole scan method. The grey bars with errorbars represent the current in each slice.

Figure 5 shows the normalized horizontal slice emittance and slice mismatch parameter obtained with (top) multi-screen method and (bottom) quadrupole scan method with the TDS operated around the RF zero-crossing. The grey bars with errorbars represent the current in each slice. The reconstructed slice emittance from these two methods shows the same tendency in the slices, with relative constant emittance in the slices with negative indices and increasing emittance values towards the positive indices. The slice mismatch parameters from these two methods show the same feature as well. The slice emittances from the multi-screen method are in general larger than that from the quadrupole scan method, which has been observed in the projected emittance measurement as well.

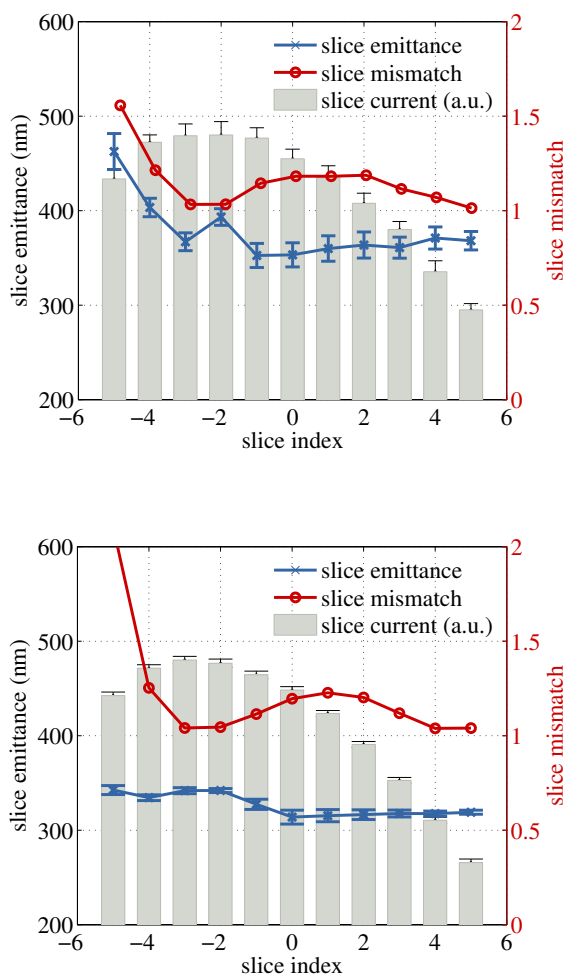


Figure 6: Normalized horizontal slice emittance and slice mismatch parameter obtained with (top) multi-screen method and (bottom) quadrupole scan method with the TDS operated around the other RF zero-crossing, i.e. with 180° phase shift compared to Fig. 5. The grey bars with errorbars represent the current in each slice.

In order to examine the influence of the TDS streak and the initial bunch correlation in ( $y'$ ,  $z$ ) on the reconstructed longitudinal distribution, we repeated the slice emittance measurement at the other TDS RF zero-crossing (see Fig. 6), i.e. with 180° phase shift compared to Fig. 5. The consistency of the reconstructed slice emittance and slice mismatch parameter derived at these two TDS RF zero-crossings is a good confirmation of our measurements and excludes the influence of an initial bunch correlation. The feature of measuring larger slice emittance from the multi-screen method than the quadrupole scan method is still observed.

Since the design twiss parameters at the reconstruction point are the same in these measurements, they can be compared as well. Table 2 summarizes the reconstructed parameters of the core slice using these two methods. Though the slice emittance measured with the multi-screen method is

larger than that with quadrupole scan, there is a good agreement between the twiss parameters, which may indicate a possible calibration error of the OTR screens. Another possible explanation for this discrepancy is the worse emittance resolution of the multi-screen method due to the smaller  $\beta$ -function at the OTR screens in the FODO cell.

Table 2: Summary of Core Slice Emittance

TDS phase	1st.	2nd.
<b>Multi-screen method</b>		
$\epsilon_{N,x}$ (nm)	$369 \pm 11$	$353 \pm 13$
$\beta_x$ (m)	$6.58 \pm 0.32$	$6.23 \pm 0.31$
$\alpha_x$	$-0.95 \pm 0.05$	$-1.03 \pm 0.04$
$B_{mag,x}$	1.10	1.18
<b>Quadrupole scan method</b>		
$\epsilon_{N,x}$ (nm)	$321 \pm 7$	$314 \pm 7$
$\beta_x$ (m)	$6.19 \pm 0.21$	$5.73 \pm 0.18$
$\alpha_x$	$-0.86 \pm 0.02$	$-0.90 \pm 0.02$
$B_{mag,x}$	1.12	1.19
$\beta_{Design,x}$ (m)	9.43	
$\alpha_{Design,x}$	-1.02	

## CONCLUSION

We have compared the projected and slice emittance using the multi-screen and quadrupole scan method at the SITF. The results are comparable and verified further by measurements at both TDS RF zero-crossings. The fact that the multi-screen method obtains generally slightly larger emittance might result from a calibration error of the OTR screens or a worse emittance resolution due to smaller  $\beta$ -function in the FODO cell.

## REFERENCES

- [1] M. Minty and F. Zimmermann, *Measurements and Control of Charged Particle Beams*, Springer, Berlin, Heidelberg, New York (2003).
- [2] J. Wychowaniak et al., "Design of TDS-based Multi-Screen Electron Beam Diagnostics for the European XFEL", THP075, *These Proceedings*, FEL'14, Basel, Switzerland (2014).
- [3] E. Prat and M. Aiba, Phys. Rev. ST Accel. Beams 17, 052801 (2014).
- [4] M. Roehrs, PhD thesis.
- [5] M. Pedrozzi et al., "250 MeV Injector Conceptual Design Report", PSI Report No. 10-05 (2010).
- [6] R. Ischebeck and V. Thominet, "Transverse Profile Imager for Ionizing Radiation", European Patent Application, EP2700979A1 (2014).
- [7] E. Prat, Nucl. Instrum. Meth. A 743, p103 (2014).
- [8] E. Prat et al., "Slice Emittance Optimization at the Swiss-FEL Injector Test Facility", FEL'13, New York, August 2013, TUOCNO06, p. 200, <http://www.JACoW.org>